AD-A043 073 NAVAL RESEARCH LAB WASHINGTON D C F/G 20/9
ROTATIONAL STABILIZATION OF THE INNER SURFACE OF A PISTON-DRIVE--ETC(U)
JUN 77 P J TURCHI, D J JENKINS, R D FORD E(49-20)-1009

UNCLASSIFIED NRL-MR-3536 NL

| OF |
AD
A043073

END
DATE
FILMED
9-77
DDC

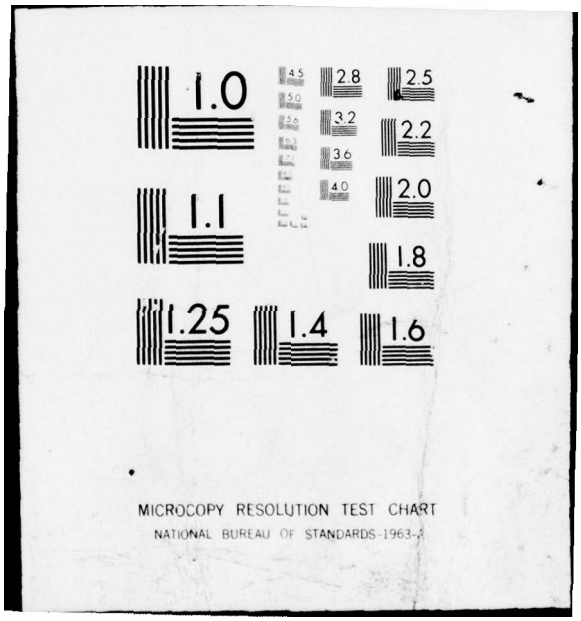
1.0
1.1
1.25
1.4
1.6
1.8
2.0
2.2
2.5
2.8
3.2
3.6
4.0
4.5
5.0
5.6
MICROCOPY RESOLUTION TEST CHART
NATIONAL BUREAU OF STANDARDS-1963-A

NRL Memorandum Report 3536

Rotational Stabilization of the Inner Surface of a Piston-Driven Imploding Liner

P. J. Turchi, D. J. Jenkins,
R. D. Ford and A. L. Cooper

Plasma Physics Division

June 1977

NAVAL RESEARCH LABORATORY
Washington, D.C.

SECURITY CLASSIFICATION OF THIS PAGE (When Data Entered)

REPORT DOCUMENTATION PAGE

READ INSTRUCTIONS BEFORE COMPLETING FORM

1. REPORT NUMBER: NRL Memorandum Report 3536

2. GOVT ACCESSION NO.

3. RECIPIENT'S CATALOG NUMBER

4. TITLE (and Subtitle): ROTATIONAL STABILIZATION OF THE INNER SURFACE OF A PISTON-DRIVEN IMPLODING LINER

5. TYPE OF REPORT & PERIOD COVERED: Interim report on a continuing NRL problem

6. PERFORMING ORG. REPORT NUMBER

7. AUTHOR(s): P.J. Turchi, D.J. Jenkins, R.D. Ford and A.L. Cooper

8. CONTRACT OR GRANT NUMBER(s): USERDA E(49-20)-1009 ED-03-02

9. PERFORMING ORGANIZATION NAME AND ADDRESS: Naval Research Laboratory, Washington, D.C. 20375

10. PROGRAM ELEMENT, PROJECT, TASK AREA & WORK UNIT NUMBERS: NRL Problem H02-28D; RR 011-09-41

11. CONTROLLING OFFICE NAME AND ADDRESS

12. REPORT DATE: June 1977

13. NUMBER OF PAGES: 27

14. MONITORING AGENCY NAME & ADDRESS (if different from Controlling Office)

15. SECURITY CLASS. (of this report): UNCLASSIFIED

15a. DECLASSIFICATION/DOWNGRADING SCHEDULE

16. DISTRIBUTION STATEMENT (of this Report)

Approved for public release; distribution unlimited.

NRL-MR-3536

17. DISTRIBUTION STATEMENT (of the abstract entered in Block 20, if different from Report)

RR011099 RR011099-1

18. SUPPLEMENTARY NOTES

19. KEY WORDS (Continue on reverse side if necessary and identify by block number)

Liner implosion
Hydrodynamic instability

20. ABSTRACT (Continue on reverse side if necessary and identify by block number)

The use of rotation to stabilize the inner surface of a liquid liner compressing a gas payload is studied experimentally. The outer surface of the liner is driven by a plurality of radially-displaced free-pistons to eliminate high frequency Rayleigh-Taylor instability at the outer surface, with the entire implosion mechanism rotating to provide angular momentum to stabilize the inner surface. Both stable and unstable inner surfaces are observed during final payload compression. Excellent correlation of observed behavior with theoretically predicted performance is obtained, providing

(Continues)

DD FORM 1 JAN 73 1473 EDITION OF 1 NOV 65 IS OBSOLETE S/N 0102-014-6601

SECURITY CLASSIFICATION OF THIS PAGE (When Data Entered)

251 950

20. Abstract (Continued)

confidence in the use of rotation to eliminate Rayleigh-Taylor instability at the inner surface of a liner compressing a lower density payload.

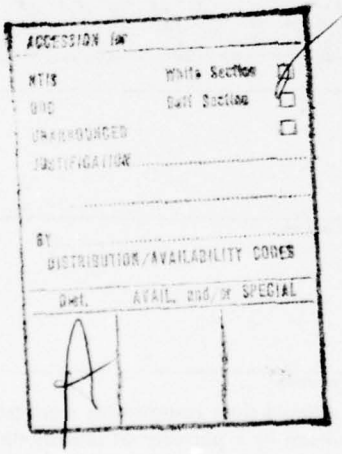

ROTATIONAL STABILIZATION OF THE INNER SURFACE OF A PISTON-DRIVEN IMPLODING LINER

The compression of a plasma and/or magnetic field by an imploding shell of higher density fluid is normally subject to Rayleigh-Taylor instability as the interface between the two fluids decelerates. Such instability can be avoided by rotating the imploding fluid so that the centripetal acceleration ($- v^2/r$) can offset the radial acceleration ($\ddot{r}$) to reverse the direction of the effective acceleration ($\ddot{r}-v^2/r$) at the interface in favor of stability. This has been shown theoretically[1,2] and has been demonstrated experimentally using electromagnetically-driven sodium-potassium liners imploding on trapped magnetic flux.[3] The use of a low density fluid (magnetic field) to accelerate the higher density liner fluid is itself subject to Rayleigh-Taylor instability, however and combines with other experimental difficulties to limit the data acquisition rate.

To study the basic hydrodynamics of rotationally stabilized liners, a lower energy density system has been used in which a plurality of radially-moving free-pistons, driven by gas pressure, inject dyed water into a central implosion chamber (Fig. 1). The entire system rotates so that the inner surface of the water forms a free circular cylinder surrounding a trapped-air payload volume. The inward motion of the pistons causes the inner surface of the

Note: Manuscript submitted May 31, 1977.

fluid to implode, thereby compressing the trapped air. Energy is transferred from stored gas energy to kinetic energy of the free-pistons and fluid, and then to the increased rotational energy of the fluid and the internal energy of the trapped-air payload. The process can reverse stably with energy flowing back to recompress the driver gas.

A schematic of the experimental arrangement used to study such stabilized implosions is shown in Fig. 2. The implosion of the inner surface is photographed using a Beckman & Whitley Model 326 fast framing camera, with the light of twenty flashbulbs reflected down into the implosion chamber and back again off an aluminum reflector to the camera. As the dyed-water liner implodes, it occults the second reflection allowing the inner surface to be delineated. Light is also reflected by the aluminum free-pistons allowing their positions to be determined. A typical, cyclic implosion sequence is shown in Fig. 3. Almost one hundred such photo sequences have been obtained in the above manner.

Of particular interest in these experiments is the verification of the criterion for rotational stabilization. This basically can be reduced to a comparison of the sign of the effective acceleration $(\ddot{r}-v^2/r)$ with the observed behavior of the liner surface. In Appendix I, the relevant formulas are derived for the radial acceleration, and centripetal acceleration in liner systems driven by radially-moving free-pistons. Defining a stability parameter, S , as

$$S = \frac{v^2/r-\ddot{r}}{v^2/r} = 1 - \frac{r\ddot{r}}{v^2} \quad ,$$

with $S \geq 0$ indicating stability of the inner surface, we have:

$$S = 1 - \frac{p_1}{\rho v_1^2} \Bigg/ \left\{ \ln \frac{r_c}{r_1} + \frac{N}{2} \left[\frac{r_p^2 x_p}{r_c^2 h_c} + \frac{M_p}{\pi \rho h_c r_c^2} \right] \right\}$$

$$- \left\{ \left(\frac{r_1}{r_i} \right)^4 \left[(r_c^2 - r_i^2) + 4(r_i^2 - r_1^2) \ln r^*/r_1 \right. \right.$$

$$+ (r_i^2 - r_1^2)(r_c^2 - r_i^2)/r_1^2 r^{*2} + r_c^4/r^{*2}$$

$$\left. \left. - (r_c + x_p)^2 - 2M_p(r_c + x_p + \Delta x_p)/\pi \rho r_p^2 \right] \right\} \Bigg/$$

$$\left\{ 2r_1^2 \left\{ \ln r_c/r_1 + \frac{N}{2} \left[\frac{r_p^2 x_p}{r_c^2 h_c} + \frac{M_p}{\pi \rho h_c r_c^2} \right] \right\} \right\}$$

where p_1 and v_1 are the payload pressure and inner surface tangential speed, respectively, at turn around, ρ is the fluid mass density and all other factors are defined in Appendix I. From numerical substitution in the situation of the present experiments, the third collection of terms can be neglected to within a few per cent, providing a much simpler formula for the stability parameter, S:

$$S = 1 - \frac{p_1}{\rho v_1^2} \Bigg/ \left\{ \ln \frac{r_c}{r_1} + \frac{N}{2} \left[\frac{r_p^2 x_p}{r_c^2 h_c} + \frac{M_p}{\pi \rho h_c r_c^2} \right] \right\}$$

Thus, for marginal stability, S = 0, the relationship between peak pressure, p_1, tangential speed at minimum radius, v_1, and the system dimensions is:

$$\frac{p_1}{\rho v_1^2} = \left\{ \ln \frac{r_c}{r_1} + \frac{N}{2} \left[\frac{r_p^2 x_p}{r_c^2 h_c} + \frac{M_p}{\pi \rho h_c r_c^2} \right] \right\} .$$

The expression in braces on the right can be rewritten as

$$\{ \quad \} = \left[\ln \frac{r_c}{r_i} + \frac{N}{2} \left[\frac{M_p}{\pi \rho h_c r_c^2} + \frac{r_p^2}{r_c^2} \frac{l_p}{h_c} \right] - \tfrac{1}{2} \left(\frac{r_i}{r_c}\right)^2 \right]$$

$$+ \ln\alpha + \tfrac{1}{2} \left(\frac{r_i}{r_c} \right)^2 / \alpha^2$$

where $\alpha = r_i / r_1$.

Note that the first group of terms in brackets depends only on the initial parameters of the experimental geometry and is independent of the compression ratio, α. If this group is labelled with the constant, c, then experiments with different values of r_i/r_c, corresponding to different thicknesses of the initial fluid annulus, can be compared simply in terms of the attained compression ratio; the last term of the expression in braces makes little contribution at significant values of α.

In Figure 4, the quantity $p_1/\rho v_1^2$-c is plotted versus α for the condition of marginal stability (S = 0). The region below the curve is associated with stability, while that above is associated with Rayleigh-Taylor instability. It should be noted that even though an experimental situation may lie above the marginal stability curve, the implosion may still appear of reasonable quality since the growth of perturbations during the final stages of implosion and turn-around may not be sufficient to destroy the surface.

From measurements of the minimum observed inside radius of liner, values can be ascertained for the payload pressure, p_1, using the adiabatic compression formula, and the tangential speed, v_1, of the inner surface material, presuming conservation of angular momentum. Using this approach, the experimental points displayed in Fig. 4 are obtained. Inspection of the photographic data indicates three classes of final implosion. The first class shows a clean and unstructured inner surface which is maintained through turn-around as shown in Fig. 5a and Fig. 6; this is described as 'stable'. The second class of implosion displays a rather total break-up of the inner surface

at turn-around, as shown in Fig. 5b and Fig. 7; this is described as 'unstable'. A third class exists in which an overall reversal of the fluid motion is observed through turn-around, but the inner surface is obscure in the form of a double variation in film exposure, and usually a change in exposure level throughout the payload region after turn-around. Two aspects of this situation from different implosion tests are displayed in Figs. 5c and in 8 and 9, indicating the growth of surface perturbations followed by a structured 'halo' surface surrounding the payload region; this class of implosion is described as 'obscure'. In that liner material penetrates the payload volume in both the latter two classes, it may be reasonable, in an operational sense, simply to describe them both as unstable, with differences in the initial perturbation spectrum accounting for differences in the final behavior. If only low mode number perturbations are available, some portion of the payload volume may remain clear, in the manner indicated by Book and Winsor,[1] even though the implosion is unstable.

With these definitions, Fig. 4 indicates excellent correlation of the experimental observations with the stabilization condition derived theoretically. All those implosions which lie below the theoretical curve and are expected to be stable are observed to be stable. For the unstable implosions which do not provide a turn-around radius, their location in Fig. 4 is determined by using the minimum radius observed prior to the destruction of the inner surface. Since $p_1/\rho v_1^2 \sim \alpha^{0.8}$, the lower value of α used in this calculation provides data points closer to the marginal stability curve than would actually occur in the absence of Rayleigh-Taylor instability.

To indicate the sensitivity of the correlation of theory and experiment to errors in the delineation of the inner surface radius, broken-lines are drawn from several of the data points to positions closer to the theoretical curve that would be allowed by the measurements. Note that, with the exception of one 'obscure' case that lies almost on the theory curve, difficulties in determining the fluid surface do not affect the correlation in terms of stable and unstable implosions.

The experimental observations and their correlation with the theoretically predicted marginal-stability curve provide considerable further confidence that rotation can be used to prevent Rayleigh-Taylor instability at the decelerating inner surface of a liquid liner implosion. These experiments are, of course, in a fluid regime in which material compression is quite small, as were the earlier electromagnetically-imploded NaK liner tests.[3] Since rotational stabilization is basically a kinematic process, however, the correlation of theory and experiment should remain good even at higher energy densities. While rotational stabilization itself may no longer be reasonably in doubt, there remain important questions involving the distribution of fluid and payload energies in high compression ratio, high energy density implosion systems. Furthermore, the use of rotation to stabilize implosion surfaces that are shaped to compress payloads in three-dimensions is of considerable interest. To study rotational stabilization at higher energy density merely requires the appropriate high energy apparatus; while the use of stabilized shaped-liner surfaces can be pursued in lower energy density hydrodynamic experiments similar to those of the present work.

APPENDIX I

Rotational Stabilization Formula for Radially-Driven Piston Liner-Implosion System

Consider a system in which N pistons travel in channels of length l_p and radius r_p, to inject fluid into an implosion chamber of height, h_c, and radius r_c. Allow an initial fluid annulus of radial thickness, δ, to provide smooth injection conditions and denote the inner radius of the fluid surface by r_1. From conservation of the incompressible fluid volume:

$$N\pi r_p^2 l_p + h_c\pi \left[r_c^2 - (r_c-\delta)^2\right]$$

$$= N\pi r_p^2 x_p + h_c\pi \left[r_c^2 - r_1^2\right] ,$$

where x_p is the length of fluid in the piston channels when the inner fluid surface is at r_1. Thus,

$$x_p = l_p - \frac{h_c}{N} \frac{\left[(r_c-\delta)^2 - r_1^2\right]}{r_p^2}$$

and $$\frac{dx_p}{dr_1} = \frac{2h_c r_1}{Nr_p^2} .$$

The total kinetic energy associated with the radial motion of the fluid is:

$$E_K = \pi\rho h_c u_1^2 r_1^2 \ln r_c/r_1 + \frac{N}{2}\left[\pi r_p^2 x_p \rho + M_p\right] \frac{u_1^2 r_1^2}{r_c^2}$$

where ρ is the fluid mass density,

u_1 is the inner surface radial speed

and M_p is the mass of a piston.

The rate of change of this energy related to the motion of the inner surface is:

$$\dot{E}_K = \pi\rho h_c \left\{ 2u_1\dot{u}_1 \left[r_1^2 \ln r_c/r_1\right] + u_1^3 \frac{d}{dr_1}\left[r_1^2 \ln r_c/r_1\right] \right\}$$

$$+ Nu_1\dot{u}_1 \left[\pi r_p^2 x_p \rho + M_p \right] \frac{r_1^2}{r_c^2} + \frac{Nu_1^3}{2} \frac{d}{dr_1} \left\{ \left[\pi r_p^2 x_p \rho + M_p\right] \frac{r_1^2}{r_c^2} \right\}$$

so, at turn-around $(u_1 = 0)$

$$\frac{\dot{E}_k}{u_1} = \left\{ 2\pi\rho h_c \left[r_1^2 \ln r_c/r_1\right] + N\left[\pi r_p x_p \rho + M_p\right] \frac{r_1^2}{r_c^2} \right\} \dot{u}_1$$

The rotational energy of the radially-moving portion of the system is comprised of portions due to the initial fluid annulus, the free fluid injected from the piston channels, and the fluid (and pistons) still within the channels. The fluid of the initial annulus is defined by

$$r_1 \leq r \leq r^* = \left[r_1^2 + r_c^2 - r_i^2 \right]^{\frac{1}{2}}$$

where r_i is the initial radius of the inner surface. The tangential speed of an element of this layer at radius r' is:

$$v(r') = \frac{\omega}{r'} \left[r'^2 + (r_i^2 - r_1^2) \right]$$

so the total rotational energy in the annulus portion is:

$$E_{RA} = \pi \rho h_c \omega^2 \int_{r_1}^{r^*} \left[r'^2 + (r_i^2 - r_1^2)\right]^2 \frac{r'dr'}{r'^2}$$

$$= \pi \rho h_c \omega^2 \int_{r}^{r^*} \left(r'^3 + 2(r_i^2 - r_1^2)r' + \frac{(r_i^2 - r_1^2)^2}{r'}\right) dr'$$

$$= \pi \rho h_c \omega^2 \left\{ \tfrac{1}{4}(r^{*4} - r_1^4) + (r_i^2 - r_1^2)(r^{*2} - r_1^2) + (r_i^2 - r_1^2)^2 \ln \frac{r^*}{r_1} \right\}$$

With $\frac{dr^*}{dr_1} = \frac{r_1}{r^*}$,

$$\frac{\dot{E}_{RA}}{u_1} = \pi \rho h_c \omega^2 \left\{ (r^{*3} \frac{r_1}{r^*} - r_1^3) + (r_c^2 - r_i^2)(-2r_1) \right.$$

$$+ 2(r_i^2 - r_1^2)(-2r_1) \ln r^*/r_1$$

$$\left. + (r_i^2 - r_1^2)^2 \left[\frac{r_1}{r^*} \left(\frac{1}{r_1} \frac{r_1}{r^*} - \frac{r^*}{r_1^2} \right) \right] \right\}$$

$$= \pi \rho h_c \omega^2 \left\{ (r^{*2} - r_1^2) r_1 - 2r_1 \left[(r_c^2 - r_1^2) + 2(r_i^2 - r_1^2) \ln r^*/r_1 \right] \right.$$

$$\left. - \frac{(r_i^2 - r_1^2)^2}{r_1 r^{*2}} (r_c^2 - r_i^2) \right\}$$

The rotational energy of the free fluid injected from the piston channels is:

$$E_{RF} = \pi\rho h_c \omega^2 r_c^4 \int_{r^*}^{r_c} \frac{r'dr'}{r'^2} = \pi\rho h_c \omega^2 r_c^4 \ln \frac{r_c}{r^*}$$

So,

$$\frac{\dot{E}_{RF}}{u_1} = \pi\rho h_c \omega^2 r_c^4 \left(\frac{r^*}{r_c}\right) \left(\frac{-r_c}{r^{*2}}\right) \frac{r_1}{r^*}$$

$$= -\pi\rho h_c \omega^2 r_c^4 \frac{r_1}{r^{*2}}$$

The rotational energy of the fluid remaining in the piston channels is:

$$E_{RC} = \frac{\rho\pi r_p^2}{2} N \int_o^{x_p} \omega^2 (r_c + x)^2 dx$$

$$= \frac{\rho\pi r_p^2 N\omega^2}{2} \int_{r_c}^{r_c + x_p} y^2 dy$$

$$= \frac{1}{6} \rho\pi r_p^2 N\omega^2 \left[(r_c + x_p)^3 - r_c^3 \right]$$

Thus,

$$\frac{\dot{E}_{RC}}{u_1} = \tfrac{1}{2}\rho\pi r_p^2 N\omega^2 (r_c + x_p)^2 \left(\frac{2h_c r_1}{Nr_p^2}\right)$$

$$= \rho\pi h_c \omega^2 (r_c + x_p)^2 r_1$$

The rotational energy of the pistons is

$$E_{RP} = \tfrac{1}{2} NM_p\omega^2 (r_c + x_p + \Delta x_p)^2 ,$$

where Δx_p is an adjustment for the finite radial extent of the pistons, so

$$\frac{\dot{E}_R}{u_1} = NM_p\omega^2 (r_c + x_p + \Delta x_p) \left(\frac{2h_c r_1}{Nr_p^2}\right) = \frac{2M_p\omega^2 h_c r_1}{r_p^2}(r_c + x_p + \Delta x_p)$$

The trapped-gas payload has an internal energy:

$$E_p = \frac{p_1}{\gamma-1} \pi r_1^2 h_c$$

$$= \frac{p_i}{\gamma-1} \pi r_1^2 h_c \left(\frac{r_i}{r_1}\right)^{2\gamma}$$

$$= \frac{p_i \pi r_i^2 h_c}{\gamma-1} \left(\frac{r_i}{r_1}\right)^{2(\gamma-1)}$$

where p_i is the initial pressure of the payload. We then have:

$$\frac{\dot{E}_p}{u_1} = \frac{p_i \pi r_i^2 h_c}{\gamma-1} \; 2(\gamma-1) \left(\frac{r_i}{r_1} \right)^{2\gamma-3} \left(\frac{-r_i}{r_1^2} \right)$$

$$= -2\pi h_c \frac{p_i r_i^3}{r_1^{2\gamma-1}} \; (r_i)^{2\gamma-3} = -2\pi h_c p_i r_i \left(\frac{r_i}{r_1} \right)^{2\gamma-1}$$

Collecting the several contributions to $\dot{E}/u_1$, we have:

$$\frac{\dot{E}_K + \dot{E}_R + \dot{E}_p}{u_1} = 0$$

$$= \left\{ 2\pi\rho h_c \left[r_1^2 \ln \frac{r_c}{r_1} \right] + N \left[\pi r_p^2 x_p \rho + M_p \right] \frac{r_1^2}{r_c^2} \right\} \dot{u}_1$$

$$+ \pi\rho h_c \omega^2 \left\{ (r_c^2 - r_i^2) r_1 - 2r \left[(r_c^2 - r_i^2) + 2(r_i^2 - r_1^2) \ln r^*/r_1 \right] \right.$$

$$\left. - (r_i^2 - r_1^2)^2 \; (r_c^2 - r_i^2)/r_1 r^{*2} \right\}$$

$$- \pi\rho h_c \omega^2 r_c^4 r_1 / r^{*2} + \rho\pi h_c \omega^2 \; (r_c + x_p)^2 \; r_1$$

$$+ 2M_p \omega^2 h_c r_1 (r_c + \Delta x_p + x_p)/r_p^2 - 2\pi h_c p_i r_i \left(\frac{r_i}{r_1} \right)^{2\gamma-1}$$

which provides the instantaneous acceleration of the inner surface at turn-around in terms of the various geometric parameters, pressure, and masses.

The condition for rotational stabilization of the inner surface at turn-around is that:

$$\frac{v^2}{r} \geq \dot{u}_1$$

Define a stabilization parameter $S = 1 - \dot{u}_1 r/v^2$, against which experimental data can be compared. With,

$$\frac{v^2}{r} = \frac{1}{r_1} (\omega r_i \frac{r_i}{r_1})^2$$

$$= \frac{\omega^2 r_i^4}{r_1^3} ,$$

we have:

$$S = 1 - \frac{p_1}{\rho v_1^2} \Bigg/ \left\{ \ln \frac{r_c}{r_1} + \frac{N}{2} \left[\frac{r_p^2 x_p}{r_c^2 h_c} + \frac{M_p}{\pi \rho h_c r_c^2} \right] \right\}$$

$$- \left\{ \left(\frac{r_1}{r_i} \right)^4 \left[(r_c^2 - r_i^2) + 4(r_i^2 - r_1^2) \ln r^*/r_1 \right. \right.$$

$$+ (r_i^2 - r_1^2)(r_c^2 - r_i^2)/r_1^2 r^{*2} + r_c^4/r^{*2}$$

$$\left. \left. - (r_c + x_p)^2 - 2M_p (r_c + x_p + \Delta x_p)/\pi \rho r_p^2 \right] \right\} \Bigg/$$

$$\left\{ 2r_1^2 \left\{ \ln r_c/r_1 + \frac{N}{2} \left[\frac{r_p^2 x_p}{r_c^2 h_c} + \frac{M_p}{\pi \rho h_c r_c^2} \right] \right\} \right\}$$

ACKNOWLEDGEMENTS

The authors express their gratitude to W. C. Bliven, R. Crosariol and R. McCarthy for technical assistance in performing the experiments, and to E. Fuliehan, Potomac Research, Inc., for assistance on the engineering design of the apparatus.

References

1. D. L. Book and N. K. Winsor, Phys. Fluids 17, 662 (1974).

2. A. Barcilon, D. L. Book, and A. L. Cooper, Phys. Fluids 17, 1707 (1974).

3. P. J. Turchi, A. L. Cooper, R. Ford, and D. J. Jenkins, Phys. Rev. Lett., 36, 1546 (1976).

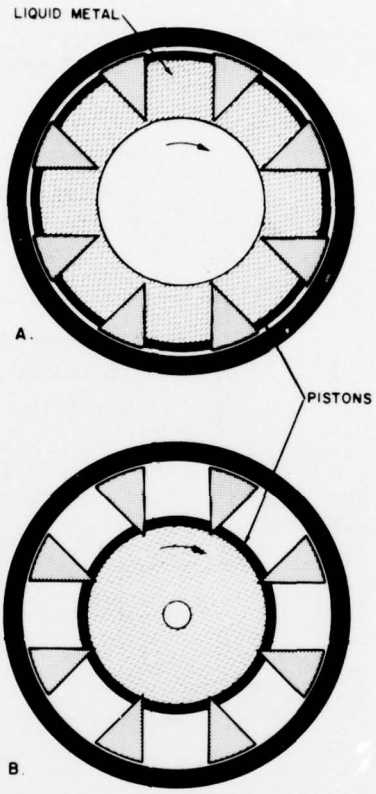

Fig. 1 — Stabilized liquid liner implosion with rotation and piston drive
(a) initial or final state and (b) imploded state (turn-around)

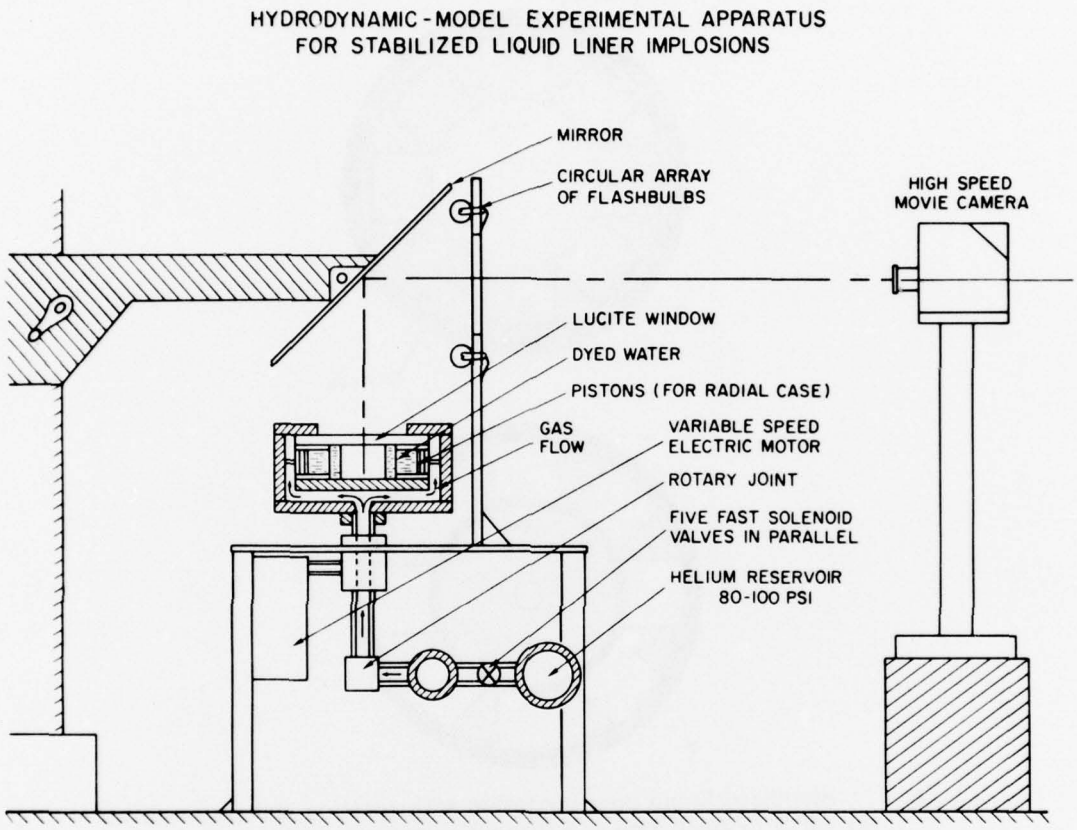

Fig. 2 — Schematic of experimental apparatus used to study stabilized liquid liner implosions. Radial piston-displacement configuration is shown, with high pressure helium gas-drive.

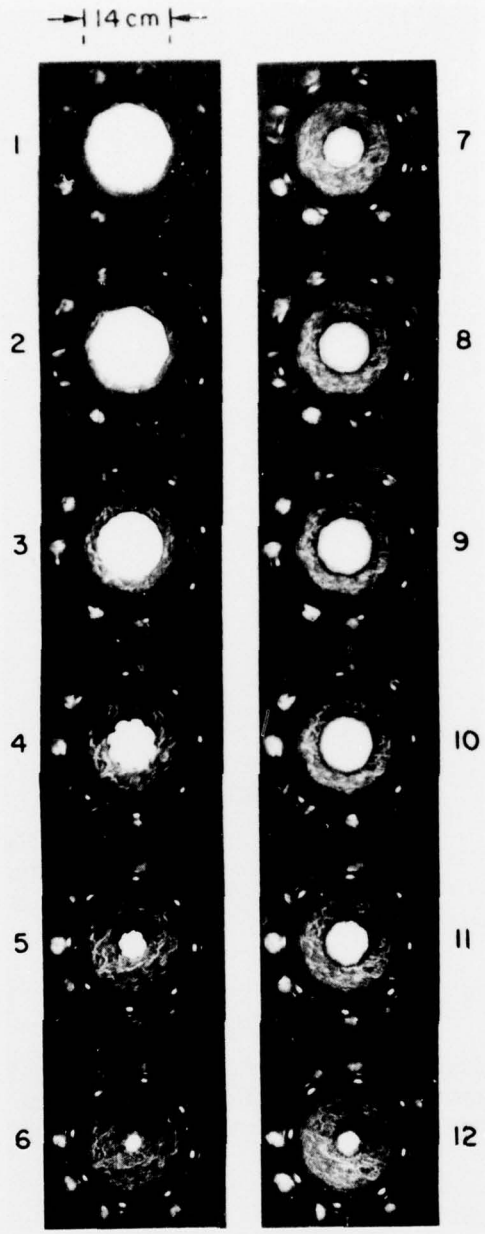

Fig. 3 — Sequence of high speed movie photographs of stabilized liquid liner behavior. Eight piston radial-drive with 1 cm initial fluid annulus. Time interval between frames is 1 msec.

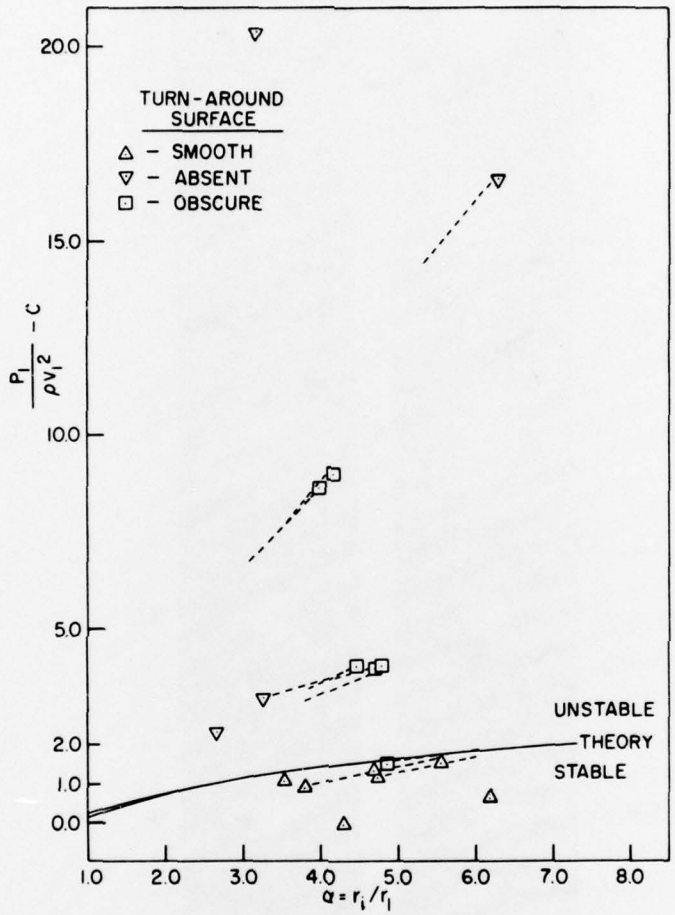

Fig. 4 — Stability diagram for piston-driven rotating liquid liner implosions. Theory and experiment are for radial-displacement pistons. The parameter c and the theory curve at low values of α depend on the buffer thickness, δ.

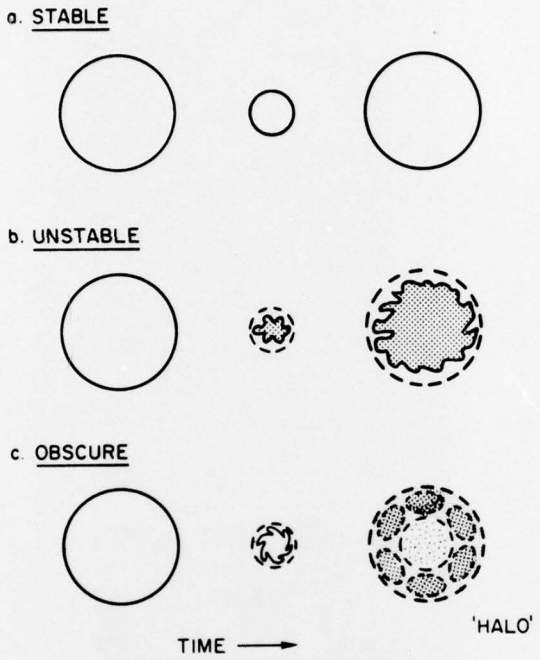

Fig. 5 — Three classes of liner implosion, showing the inner liner surface near minimum radius

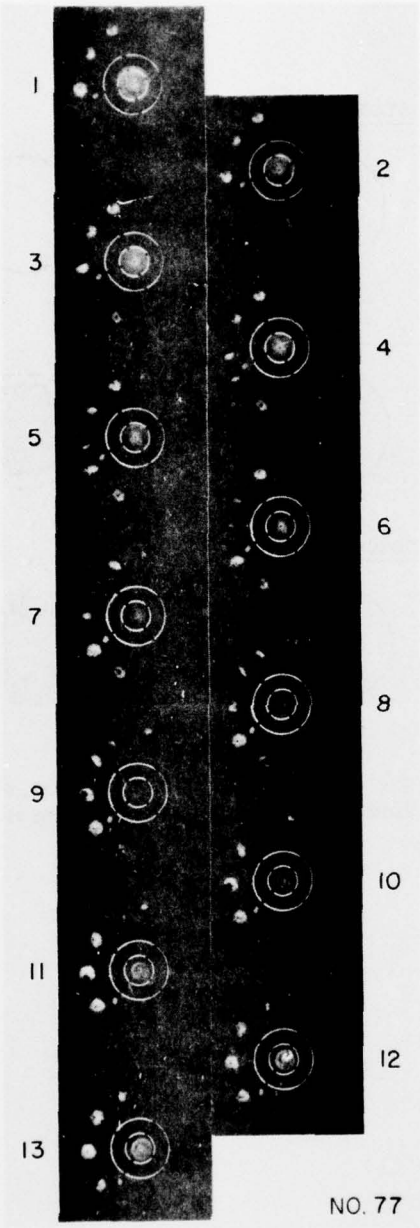

Fig. 6 — High speed photo sequence of 'stable' liner implosion. Outside edge of outermost fiducial circle is 11.05 cm diam. Time between integer frames is 621 μsec

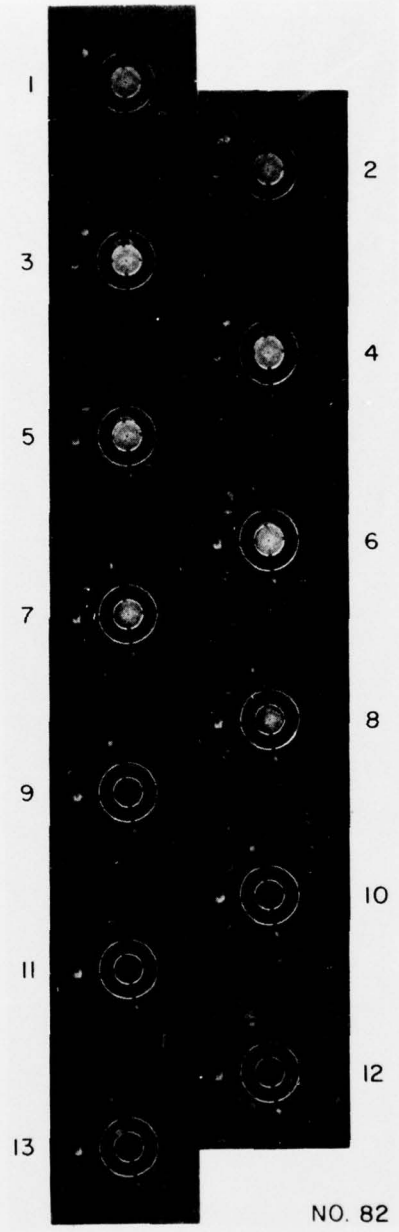

Fig. 7 — High speed photo sequence of 'unstable' liner implosion. Outside edge of outermost fiducial circle is 11.05 cm diam. Time between integer frames is 616 μsec.

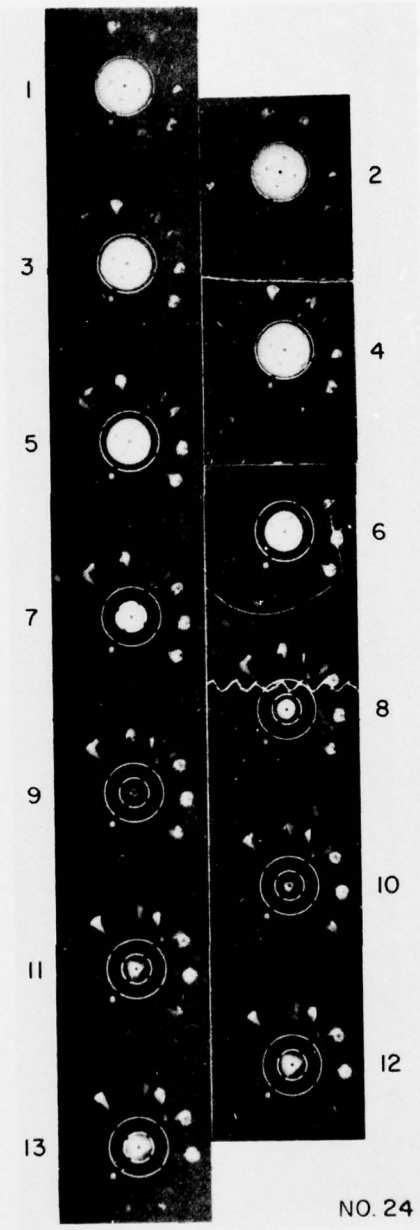

Fig. 8 — High speed photo sequence of 'obscure' liner implosion, showing development and breaking of surface waves. Outside edge of outermost fiducial circle is 11.05 cm diam. Time between integer frames is 576 μsec. Frames 2 and 4 should precede 1 and 3 to account for missing frame of right-hand of film strip.

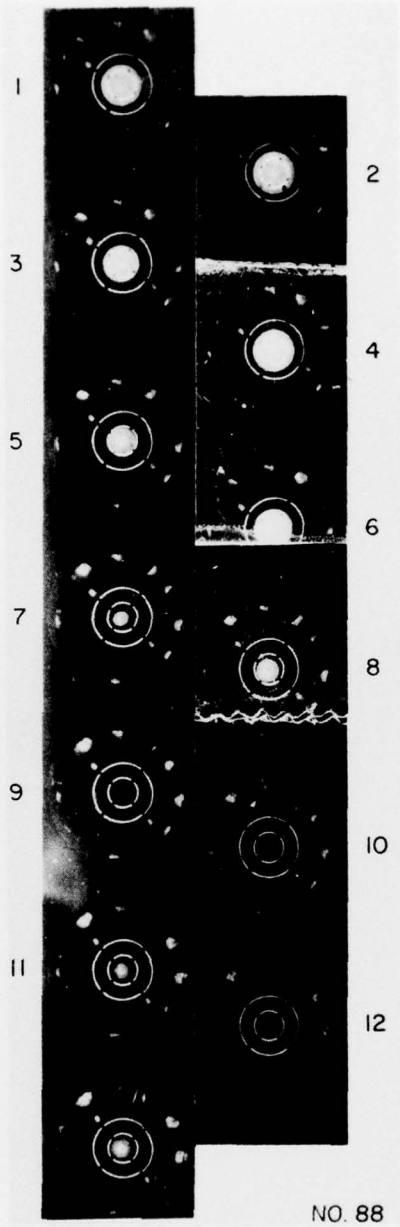

Fig. 9 — High speed photo sequence of 'obscure' liner implosion, showing "halo" surface after minimum radius. Outside edge of outermost fiducial circle is 11.05 cm diam. Time between integer frames is 621 μsec. Right-hand film strip should be shifted up one frame to correct processing error.